

# Solvable model of a phase oscillator network on a circle with infinite-range Mexican-hat-type interaction

Tatsuya Uezu<sup>1,\*</sup>, Tomoyuki Kimoto<sup>2</sup>, and Masato Okada<sup>3</sup>

<sup>1</sup>*Graduate School of Humanities and Sciences, Nara Women's University, Nara 630-8506, Japan*

<sup>2</sup>*Oita National College of Technology, Oita 870-0152, Japan*

<sup>3</sup>*Graduate School of Frontier Sciences, The University of Tokyo, Kashiwa, Chiba 277-8561, Japan*

(Dated: May 8, 2019)

We describe a solvable model of a phase oscillator network on a circle with infinite-range Mexican-hat-type interaction. We derive self-consistent equations of the order parameters and obtain three non-trivial solutions characterized by the rotation number. We also derive relevant characteristics such as the location-dependent distributions of the resultant frequencies of desynchronized oscillators. Simulation results closely agree with the theoretical ones.

**PACS numbers:** 05.45.Xt 05.45.-a 05.20.-y 87.10.Rt

It is ubiquitously observed in nature that a system composed of many active elements exhibits collective behavior as a whole. A typical example is the synchronization of populations of oscillators, e.g., simultaneous emission of light by fireflies, the rhythm of the heart composed of a population of cardiac muscle cells, and circadian rhythms [1, 2].

Pioneering studies on such behavior were done by Winfree [3] and Kuramoto [4]. In particular, Kuramoto regarded synchronization as a phase transition and described a prototype model of the phase transition in non-equilibrium systems. The model, today called the “Kuramoto model,” is a coupled oscillator system in which an oscillator interacts with all other oscillators with the same strength. Each oscillator has its own natural frequency, but its amplitude is constant and the state variable is its phase. In general, when nonlinear dynamical systems with stable limit cycle oscillators are weakly coupled, the whole system can be described by the phases of the oscillators, and the dynamical equation is reduced to the evolution equation for phases [4]. The Kuramoto model was used to analytically prove for the first time that, as the interaction strength increases from zero, a phase transition occurs, from a desynchronized state in which each oscillator independently oscillates with its own frequency to a synchronized state in which a large number of oscillators oscillate with the same frequency [5]. Since Kuramoto’s analysis of globally coupled oscillators, oscillator networks with short-range and with intermediate-range interactions have been studied [6]. Oscillators with global and random interactions [7] and with sparse and random interactions [8] have also been studied. Furthermore, the stability of the solutions with the Kuramoto model has been studied [9, 10]. A review of the Kuramoto model and its extensions, such as inclusion of a noise term, is available elsewhere [11]. There have also been extensive studies on the statistical and dynamical

properties of the mean-field XY model (HMF XY model) of conservative dynamical systems corresponding to oscillator network models of dissipative dynamical systems [12, 13].

Although there have been many studies on oscillator networks, no solvable model defined in a finite-dimensional space has yet been introduced. It is greatly difficult to study systems with short- and intermediate-range interactions analytically, so we cannot help relying on numerical simulation to study such systems. To further advance the study of the synchronization–desynchronization transition of active elements, it is quite desirable to introduce a solvable model that extends the Kuramoto model.

In this paper, we describe a phase oscillator network on a circle, and, to make analytical treatment possible, we assume infinite-range interaction and that the strength and sign of the interaction between two oscillators depend on the spatial distance between them. We specifically adopt the Mexican-hat-type interaction, which was introduced to model the creation of feature extraction cells in neuroscience and expresses the properties that a firing cell excites nearby cells and inhibits distant cells [14]. For an XY model on a circle with this interaction, it was found that there exists a peculiar solution, the pendulum solution, in which the phases of the XY spins do not rotate but oscillate as the locations change on the circle [15]. In the phase oscillator network, we show that the self-consistent equations (SCEs) of the order parameters for stationary states and the relevant quantities can be exactly derived theoretically, and that there exists a pendulum solution as in the XY model.

Now we explain the phase oscillator network. Let  $\phi_i$  and  $\theta_i$  be the phase and location on the circle of the  $i$ -th oscillator. We regard the  $i$ -th oscillator as a two-dimensional vector,  $\mathbf{X}_i = (\cos \phi_i, \sin \phi_i)$ . We assume that oscillators are located uniformly on the circle; that is,  $\theta_i = i2\pi/N$  ( $i = 0, \dots, N-1$ ). The evolution equation

\* uezu@ki-rin.phys.nara-wu.ac.jp

for the  $i$ -th phase is

$$\frac{d}{dt}\phi_i = \omega_i + \frac{1}{N} \sum_j J_{ij} \sin(\phi_j - \phi_i), \quad (1)$$

which is derived under the rather general situation described above. Here,  $\omega_i$  is the natural frequency and is drawn from the probability density  $g(\omega)$ , which is assumed to be one-humped at  $\omega = \omega_0$  and symmetric with respect to  $\omega_0$ . In our numerical simulations, we used a Gaussian distribution  $g(\omega)$  with a mean of zero and a standard deviation  $\sigma$ .

Let us explain the interaction we use in this paper in detail. We impose translational symmetry on  $J_{ij}$ , i.e.,  $J_{ij}$  takes the form  $J_{ij} = J(\theta_i - \theta_j)$ . Furthermore, we assume  $J_{ij} = J_{ji}$ . Thus,  $J(\theta)$  is an even function of  $\theta$ . Therefore, the Fourier expansion of  $J(\theta)$  is given by

$$J(\theta) = J_0 + J_1 \cos(\theta) + J_2 \cos(2\theta) + \dots \quad (2)$$

In this study, we treat the case in which only  $J_0$  and  $J_1$  are non-zero, so the interaction is

$$J_{ij} = J_0 + J_1 \cos(\theta_i - \theta_j), \quad (3)$$

which has the properties expressed by the Mexican-hat-type interaction described above.

The order parameters are defined as

$$Re^{i\Theta} = \frac{1}{N} \sum_j e^{i\phi_j},$$

$$R_c e^{i\Theta_c} = \frac{1}{N} \sum_j \cos \theta_j e^{i\phi_j}, \quad R_s e^{i\Theta_s} = \frac{1}{N} \sum_j \sin \theta_j e^{i\phi_j}.$$

Using these order parameters, we rewrite the evolution equation (1) as

$$\begin{aligned} \frac{d}{dt}\phi_i &= \omega_i + J_0 R \sin(\Theta - \phi_i) \\ &+ J_1 [R_c \cos \theta_i \sin(\Theta_c - \phi_i) + R_s \sin \theta_i \sin(\Theta_s - \phi_i)]. \end{aligned} \quad (4)$$

Now we derive the SCEs. Without loss of generality, we assume  $\omega_0 = 0$ . Since we study stationary states, let us assume that amplitudes and phases tend to constant values as  $t$  tends to infinity. We further rewrite eq. (4) as

$$\frac{d}{dt}\phi_j = \omega_j - A_j \sin(\phi_j - \alpha_j). \quad (5)$$

The following relation is derived from a comparison of eqs. (4) and (5):

$$A_j e^{i\alpha_j} = J_0 R e^{i\Theta} + J_1 [R_c \cos \theta_j e^{i\Theta_c} + R_s \sin \theta_j e^{i\Theta_s}] \quad (6)$$

Hereafter, we use  $\theta$  to identify each oscillator, so  $A_\theta$  is expressed as

$$\begin{aligned} A_\theta^2 &= (J_0 R)^2 + J_1^2 \{ (R_c \cos \theta)^2 + (R_s \sin \theta)^2 \\ &+ 2R_c R_s \cos(\tilde{\Theta}_c - \tilde{\Theta}_s) \sin \theta \cos \theta \} \\ &+ 2J_0 J_1 R \{ R_c \cos \tilde{\Theta}_c \cos \theta + R_s \cos \tilde{\Theta}_s \sin \theta \}, \end{aligned} \quad (7)$$

where  $\tilde{\Theta}_c \equiv \Theta_c - \Theta$ ,  $\tilde{\Theta}_s \equiv \Theta_s - \Theta$ . Defining  $\psi_\theta \equiv \phi_\theta - \alpha_\theta$  transforms the evolution equation into

$$\frac{d}{dt}\psi_\theta = \omega_\theta - A_\theta \sin \psi_\theta. \quad (8)$$

From this equation, we can develop a theory by following Kuramoto's argument. For the synchronized oscillators satisfying  $|\omega_\theta| \leq A_\theta$ , we obtain the entrained phase  $\psi_\theta^*$  and the number density of the synchronized oscillators with the value of phase  $\psi$  at location  $\theta$ ,  $n_s(\theta, \psi)$ , as

$$\psi_\theta^* = \text{Sin}^{-1}\left(\frac{\omega_\theta}{A_\theta}\right), \quad (9)$$

$$n_s(\theta, \psi) = g(A_\theta \sin \psi) A_\theta \cos \psi, \quad |\psi| \leq \frac{\pi}{2}, \quad (10)$$

where  $\text{Sin}^{-1}x$  is the principal value and its range is  $[-\frac{\pi}{2}, \frac{\pi}{2}]$ . For the desynchronized oscillators satisfying  $|\omega_\theta| > A_\theta$ , we obtain the solution of differential equation (8) and the number density of the desynchronized oscillators with the value of phase  $\psi$  at location  $\theta$ ,  $n_{ds}(\theta, \psi)$ , as

$$\psi_\theta = \tilde{\omega}_\theta t + h(\tilde{\omega}_\theta t), \quad (11)$$

$$\tilde{\omega}_\theta = \omega_\theta \sqrt{1 - \left(\frac{A_\theta}{\omega_\theta}\right)^2}, \quad (12)$$

$$n_{ds}(\theta, \psi) = \frac{1}{\pi} \int_{A_\theta}^{\infty} dx x g(x) \frac{\sqrt{x^2 - A_\theta^2}}{x^2 - A_\theta^2 \sin^2 \psi}, \quad (13)$$

where  $\tilde{\omega}_\theta$  is the resultant frequency and  $h(t)$  is a periodic function of  $t$  with period  $2\pi$ . Note that the entrained phases and the distribution of resultant frequencies depend on the oscillator locations, in general. From eq. (13),  $n_{ds}(\theta, \psi + \pi) = n_{ds}(\theta, \psi)$  is derived, and  $\int_0^{2\pi} n_{ds}(\theta, \psi) e^{i\psi} d\psi = 0$  follows. Thus, only the synchronized oscillators contribute to the order parameters:

$$Re^{i\Theta} = \int_{-\pi}^{\pi} d\psi n_s(\psi) e^{i\psi + i\alpha_\theta}, \quad (14)$$

$$R_c e^{i\Theta_c} = \int_{-\pi}^{\pi} d\psi \frac{1}{2\pi} \int_0^{2\pi} d\theta n_s(\theta, \psi) \cos \theta e^{i\psi + i\alpha_\theta}, \quad (15)$$

$$R_s e^{i\Theta_s} = \int_{-\pi}^{\pi} d\psi \frac{1}{2\pi} \int_0^{2\pi} d\theta n_s(\theta, \psi) \sin \theta e^{i\psi + i\alpha_\theta}, \quad (16)$$

where  $n_s(\psi) = \frac{1}{2\pi} \int_0^{2\pi} d\theta n_s(\theta, \psi)$ . Substituting the expression for  $n_s(\theta, \psi)$  into these equations, and after some algebra, from the real parts of these equations, we obtain

$$R = J_0 R \langle 1 \rangle + J_1 (R_c f \cos \tilde{\Theta}_c + R_s g \cos \tilde{\Theta}_s), \quad (17)$$

$$R_c = J_0 R f \cos \tilde{\Theta}_c + J_1 \{ R_c a + R_s c \cos(\tilde{\Theta}_c - \tilde{\Theta}_s) \}, \quad (18)$$

$$R_s = J_0 R g \cos \tilde{\Theta}_s + J_1 \{ R_c c \cos(\tilde{\Theta}_c - \tilde{\Theta}_s) + R_s b \}, \quad (19)$$

$$a = \langle \cos^2 \theta \rangle, \quad b = \langle \sin^2 \theta \rangle, \quad c = \langle \sin \theta \cos \theta \rangle,$$

$$f = \langle \cos \theta \rangle, \quad g = \langle \sin \theta \rangle,$$

$$\langle B \rangle = \frac{1}{\pi} \int_0^{\pi/2} d\psi \int_0^{2\pi} d\theta g(A_\theta \sin \psi) \cos^2 \psi B.$$

These are the SCEs for  $R$ ,  $R_c$ , and  $R_s$ . Furthermore, we derive the following auxiliary equations from the imaginary parts of eqs. (14)-(16):

$$J_0 R f \sin \tilde{\Theta}_c + J_1 R_s c \sin(\tilde{\Theta}_c - \tilde{\Theta}_s) = 0, \quad (20)$$

$$J_0 R g \sin \tilde{\Theta}_s - J_1 R_c c \sin(\tilde{\Theta}_c - \tilde{\Theta}_s) = 0. \quad (21)$$

From these equations, the phases of the order parameters are completely determined. The detailed results will be reported elsewhere. There are four solutions of the SCEs, and they are classified on the basis of the values of  $R$  and  $R_1 = \sqrt{R_c^2 + R_s^2}$  as

P: para magnetic solution,  $(R, R_1) = (0, 0)$ ,

U: uniform solution,  $(R, R_1) = (+, 0)$ ,

S: spinning solution,  $(R, R_1) = (0, +)$ ,

Pn: pendulum solution,  $(R, R_1) = (+, +)$ .

Now, let us consider the physical meanings of these solutions. To characterize the solutions further, we define the rotation number of a solution. The rotation number is the number of rotations of synchronized oscillator  $\mathbf{X}_\theta^* = (\cos \phi_\theta^*, \sin \phi_\theta^*)$  around the origin in space  $\mathbf{X}$  as location  $\theta$  changes by  $2\pi$ . In the P solution, all oscillators desynchronize, whereas in the other three solutions, an extensive number of oscillators synchronize and their directions are locked. In the U solution,  $\phi_\theta^*$  randomly takes a value in the interval  $[-\frac{\pi}{2} + \Theta, \frac{\pi}{2} + \Theta]$  irrespective of the location of the oscillator, so the rotation number is 0. In the S solution,  $\phi_\theta^*$  linearly depends on  $\theta$ , and the rotation number is 1. In the Pn solution,  $\phi_\theta^*$  fluctuates and the rotation number is 0. See Figs. 1(a)-(c).

We display the phase diagram in the scaled parameter

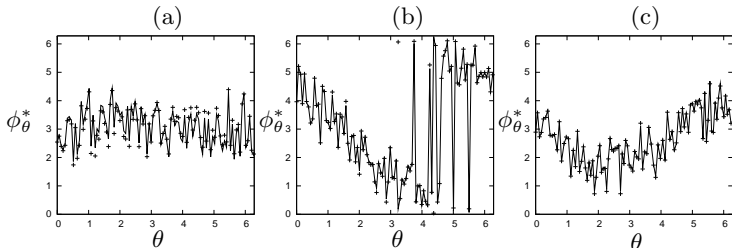


FIG. 1.  $\theta$  dependencies of entrained phases  $\phi_\theta^*$ . Line plots: theory; +: simulation ( $N = 10000, \sigma = 0.2, J_0 = 1.2J_{0,c}$ ). Only 1% of entrained phases are depicted. (a) U solution,  $J_1/J_0 = 1.9$ , (b) S solution,  $J_1/J_0 = 2.1$ , (c) Pn solution,  $J_1/J_0 = 2.1$ .

space  $(J_0/\sigma, J_1/\sigma)$  in Fig. 2(a).

Let us examine the bifurcation structures. As shown in the phase diagram in Fig. 2(a), the S and U solutions and the S and Pn solutions can coexist. We display the  $J_1/\sigma$  dependencies of order parameters  $R$  and  $R_1$  with  $J_0/\sigma$  fixed to 4 in Fig. 2(b). These results show that the unstable Pn solution determines the boundary of the coexistent regions of the S and U solutions and that of the S and Pn solutions. Furthermore, we note that the Pn solution continuously bifurcates from the U solution.

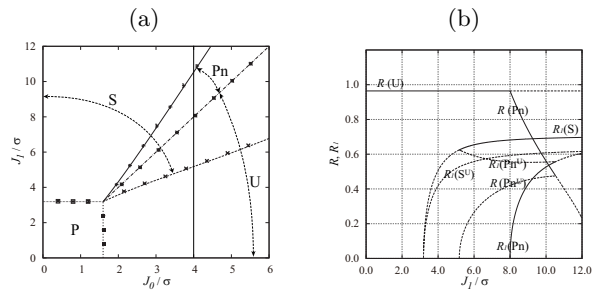


FIG. 2. (a) Phase diagram in scaled parameter space. Plot points represent simulation results; curves represent theoretical results. Vertical line represents parameters shown in (b). (b)  $J_1/\sigma$  dependencies of order parameters.  $J_0/\sigma = 4$ . Solid curves represent stable solutions; dashed curves represent unstable solutions, which have superscript U, e.g.,  $S^U$ .

Taking into account these observations, we derived the formulas for the boundaries of bistable regions by using the unstable Pn solution and relevant stable solutions. In Fig. 2(a), the theoretically obtained boundaries are represented by curves. The theoretical results are in good agreement with the simulation results.

Now, let us examine the physical meanings of the phase transitions. There are five boundaries in the phase diagram shown in Fig. 2(a). The transition from the P to U phase takes place continuously at  $J_0 = J_{0,c} \equiv 2/(g(\omega_0)\pi)$ , and this is the same transition as in the Kuramoto model. The transition from the P to S phase takes place continuously at  $J_1 = J_{1,c} \equiv 2J_{0,c}$ . In the P phase, the rotation number is not defined while it is 1 in the S phase. The transition from the U to Pn phase takes place continuously at  $J_1 = 2J_0$ . In this case, the rotation number in both phases is 0. However, as is shown in Figs. 5(a) and (c), the directions of two synchronized oscillators do not correlate in the U phase but correlate weakly in the Pn phase because magnitude  $J_1$  of the location-dependent interaction is larger after the transition than before the transition. At the two bistable region boundaries, the stable S and unstable Pn solutions and the stable Pn and unstable Pn solutions merge, and the stable S and stable Pn solutions disappear. The unstable Pn solution differs from the paired solution of the stable Pn solution because the phases of the order parameters are different. That is, these are a new type of instability that does not exist in the Kuramoto model.

We show theoretical and numerical results for the  $J_0$

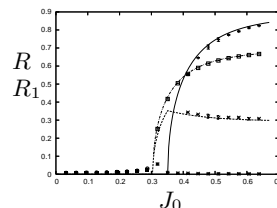


FIG. 3.  $J_0$  dependencies of order parameters.  $J_1 = 2.1J_0$ . Curves represent theory; symbols represent simulation results.  $N = 20000, \sigma = 0.2$ . Averages were taken for 20 samples. Solid curve and +:  $R$  of Pn solution; dashed curve and  $\times$ :  $R_1$  of Pn solution; dashed dotted curve and square:  $R_1$  of S solution. Vertical lines are error bars.

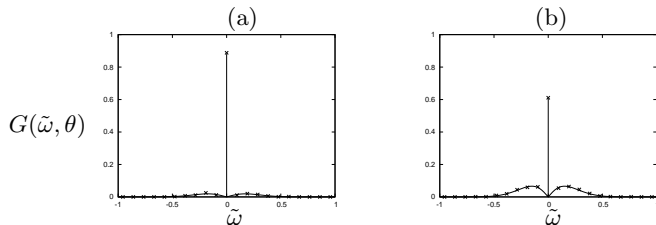


FIG. 4. Distribution  $G(\tilde{\omega}, \theta)$  of resultant frequencies for Pn solution. Curve represents theory;  $\times$  represents simulation results ( $N = 100000$ ,  $\sigma = 0.2$ ,  $J_1/J_0 = 2.1$ ,  $J_0 = 1.2J_{0,c}$ ). (a)  $\theta = 0.05 \times 2\pi$ , (b)  $\theta = 0.25 \times 2\pi$ .

dependencies of the order parameters in Fig. 3, those for the location-dependent resultant frequency distribution  $G(\tilde{\omega}, \theta)$  for different  $\theta$  for the Pn solution in Fig. 4, and those for the  $\theta$  dependencies of the entrained phases  $\phi_\theta^*$  for the U, S, and Pn solutions in Figs. 1(a)-(c). The agreement between the theoretical and numerical results is excellent. To investigate the desynchronized oscillators, we constructed a Lorenz plot of time series  $\sin(\phi_i(t))$  for the Pn solution (Fig. 5). The Lorenz plot is defined

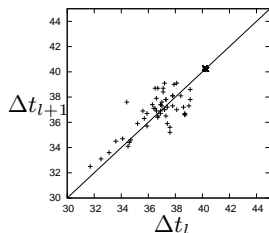


FIG. 5. Lorenz plot for desynchronized oscillator for Pn solution.  $\times$ : theory;  $+$ : simulation ( $N = 10000$ ,  $\sigma = 0.2$ ,  $J_1/J_0 = 2.1$ ,  $J_0 = 1.2J_{0,c}$ ).

as the mapping from the difference  $\Delta t_l = t_{l+1} - t_l$  to  $\Delta t_{l+1}$ , where  $t_l$  and  $t_{l+1}$  are the successive times that satisfy  $\cos(\phi_i(t_l)) = 1$  and  $\cos(\phi_i(t_{l+1})) = 1$ , respectively. As shown in Fig. 5, the simulation results are scattered in the Lorenz plot. This indicates that the trajectory of a desynchronized oscillator behaves chaotically even though theoretically it is quasi-periodic. How-

ever, in most of our numerical results, e.g., for the resultant frequency distribution, the larger the  $N$ , the better the agreement between the theoretical and numerical results. Our results suggest that the system behaves quasi-periodically in the limit of  $N$  infinity.

In summary, we have extended the Kuramoto model, which is a prototype model of the synchronization–desynchronization phase transition in non-equilibrium systems, and have proposed a solvable model of a phase oscillator network on a circle with infinite-range Mexican-hat-type interaction. We derived two auxiliary equations by expressing the order parameters by the number density of the oscillators. We used them to analytically determine the phases of the order parameters, derive self-consistent equations, and obtain three non-trivial solutions that are characterized by the order parameters and the rotation numbers of the synchronized oscillators  $\mathbf{X}_\theta^*$ s. We drew phase diagrams by using formulas for the phase boundaries derived using the unstable Pn solution, found that the unstable Pn solution differs from the paired solution of the stable synchronized solution, and the transition due to pair annihilation of the solution and the relevant solution is a new type of instability that does not exist in the Kuramoto model. We also analytically obtained the location-dependent distribution of the resultant frequencies and entrained phases and validated the theoretical results by simulation, except for the chaotic behavior of the desynchronized oscillators. Our numerical results suggest that the system behaves quasi-periodically in the limit of  $N$  infinity.

In general, when nonlinear dynamical systems that have stable limit cycle oscillators are weakly coupled, the whole system can be described by phases of oscillators, and the dynamical equation is reduced to the evolution equation for phases with general interaction  $J_{ij}$ . Therefore, by applying the present method to weakly coupled dynamical systems on a circle, we should be able to obtain new types of solutions and new types of synchronization–desynchronization phase transitions. Several such studies are now underway.

- 
- [1] D. S. Saunders, *An Introduction to Biological Rhythms* (Blackie, Glasgow and London, 1977).  
[2] A. T. Cloudsley-Thompson, *Biological Clocks—Their Function in Nature* (Weidenfeld and Nicolson, London, 1980)  
[3] A. T. Winfree, *J. Theor. Biol.* **16**, 15 (1967).  
[4] Y. Kuramoto, *Chemical Oscillations, Waves, and Turbulence* (Springer-Verlag, 1984).  
[5] Y. Kuramoto, in: Proc. Int. Symp. on Mathematical Problems in Theoretical Physics, ed. H. Araki (Springer, New York, 1975).  
[6] H. Sakaguchi, S. Shinomoto and Y. Kuramoto, *Prog. Theor. Phys. Lett.* **77**, 1005 (1987); Y. Kuramoto and H. Nakao, *Phys. Rev. Lett.* **76**, 4352 (1996).  
[7] H. Daido, *Phys. Rev. Lett.* **68**, 1073 (1992).  
[8] J. P. L. Hatchett and T. Uezu, *Phys. Rev. E* **78**, 036106 (2008); J. P. L. Hatchett and T. Uezu, *J. Phys. Soc. Jpn.*, **78**, No. 2, 024001 (2009).  
[9] R. E. Mirollo and S. H. Strogatz, *J. Stat. Phys.*, **60**, 245 (1990); R. E. Mirollo and S. H. Strogatz, *J. Nonlinear Sci.*, **17**, 309 (2007).  
[10] H. Chiba and I. Nishikawa, *Chaos*, **21**, 043103 (2011).  
[11] J. A. Acebrón, L. L. Bonilla, C. J. Pérez Vicente and F. Ritort, *Rev. Mod. Phys.* **77**, 137 (2005).  
[12] M. Antoni and S. Ruffo, *Phys. Rev. E* **52**, 2361 (1995).  
[13] A. Campa, T. Dauxois and S. Ruffo, *Phys. Rep.* **480**, 57 (2009) and papers cited therein.  
[14] D. H. Hubel and T. N. Wiesel, *J. Physiol.* **160**, 106 (1968); *ibid* **195**, 215 (1968).  
[15] T. Kimoto, T. Uezu and M. Okada, *J. Phys. Soc. Jpn.*, **80**, No. 7, 074005 (2011).